Detailed angular correlation analysis with 4π spectrometers: Spin determinations and multipolarity mixing measurements in ^{128}Ba

I. Wiedenhöver,[1,2] O. Vogel,[1] H. Klein,[1] A. Dewald,[1] P. von Brentano,[1] J. Gableske,[1] R. Krücken,[3] N. Nicolay,[1] A. Gelberg,[1] P. Petkov,[4] A. Gizon,[5] J. Gizon,[5] D. Bazzacco,[6] C. Rossi Alvarez,[6] G. de Angelis,[7] S. Lunardi,[7] P. Pavan,[6] D. R. Napoli,[7] S. Frauendorf,[8] F. Dönau,[8] R. V. F. Janssens,[2] and M. P. Carpenter[2]

[1]*Institut für Kernphysik der Universität zu Köln, 50937 Köln, Germany*

[2]*Argonne National Laboratory, 9700 South Cass Avenue, Argonne, Illinois 60439*

[3]*W. A. Wright Nuclear Structure Laboratory, Yale University, New Haven, Connecticut 06520*

[4]*Bulgarian Academy of Sciences, Institute for Nuclear Research and Nuclear Energy, 1784 Sofia, Bulgaria*

[5]*Institut des Sciences Nucléaires, Université J. Fourier, F-38036 Grenoble Cedex, France*

[6]*Dipartimento di Fisica and INFN, Sezione di Padova, Padova, Italy*

[7]*INFN, Laboratori Nazionali di Legnaro, Legnaro, Italy*

[8]*Forschungszentrum Rossendorf, D-01219 Dresden, Germany*

(Received 11 February 1998)

We analyze for the first time the full $\gamma\gamma$ directional correlations from oriented states (DCO) in an experiment performed with the GASP detector array. Our analysis is based on a transformation of the directional information into expansion coefficients of an orthogonal basis. With this method, which we call SpeeDCO (spectral expansion of DCO), the complete DCO information is concentrated in 12 $\gamma\gamma$ coincidence spectra. The analysis is applicable to all detector arrays which uniformly cover the solid angle. We show that the complete DCO information can be used for a reliable and unique determination of spins and multipolarity mixing ratios in weakly populated bands. We were able to establish the spins and the positive parity of the $\Delta I=1$ ''$M1$ band'' in ^{128}Ba and multipolarity mixing ratios of nine $M1/E2$ in-band transitions were derived as well. The measured values are in good agreement with those expected for a high-K rotational band. [S0556-2813(98)00608-6]

PACS number(s): 21.10.Re, 23.20.Lv, 25.70.Gh, 27.60.+j

I. INTRODUCTION

The xenon, barium, and cerium isotopes with mass $A \approx 130$ are well known for a variety of collective nuclear deformations. They possess γ-soft, triaxial deformation in the ground state with moderate quadrupole deformations of $\beta \approx 0.2$. Because of their γ softness, quasiparticle excitations can polarize the deformation towards prolate or oblate shapes more easily than in well-deformed nuclei. Nevertheless, the properties of these nuclei vary smoothly with mass number. One characteristic excitation in this mass region corresponds to four-quasiparticle ''$M1$ bands'' with $\Delta I=1$ transitions dominating over the competing $\Delta I=2$ ones. These structures were interpreted as a realization of ''tilted axis cranking'' (TAC) by Frauendorf and co-workers [1–3] and were as such called ''t bands.'' An alternative interpretation as high-K rotational bands was also proposed [3].

The purpose of the present work is to establish the spin, parity, and multipolarity mixing ratios $\delta(E2/M1)$ for the members of the ''$M1$ band'' in ^{128}Ba. Our analysis of $\gamma\gamma$ directional correlations from oriented states (DCO) was performed on the data set of an experiment at the GASP spectrometer at the INFN in Legnaro. The excited states of ^{128}Ba were populated in the fusion-evaporation reaction ^{96}Mo(^{36}S,4n)^{128}Ba at a beam energy of 150 MeV. The γ-triples coincidence events were recorded in two runs, from a thin and a thick target, respectively.

The level scheme and lifetime data of the experiment were published in [3]. In that work, discrete connections between the ''$M1$ band'' and the lower level scheme were established for the first time in this mass region (see Fig. 1). The experiment also provided data on branching ratios between $\Delta I=1$ and $\Delta I=2$ transitions in the ''$M1$ band'' and absolute lifetimes of three levels in this band. The comparison of transition matrix elements with the predictions of different models, such as TAC or a description as a high-K rotational band, was based on the assumption that the band has negative parity and that $\Delta I=1$ transitions have pure $M1$ character. At that time these assumptions could not be proved by experimental data. This issue was one motivation for the analysis of the DCO information described in the present work.

The evaluation of DCO is a well-known method to assign spins and parities to excited nuclear states and to measure multipolarity mixing ratios [4,5]. This method is particularly important for low-spin experiments, where spin determinations and multipolarity measurements are the central goals of the analysis [6,7]. Nevertheless, evaluating the complete DCO information has not become a standard technique for the new generation of 4π detector arrays. In a straightforward DCO analysis from these spectrometers, the experimental statistics would be spread over many spectra of different geometrical angles, e.g., 107 spectra for the geometry of GASP [8] or even 320 spectra for GAMMASPHERE [9].

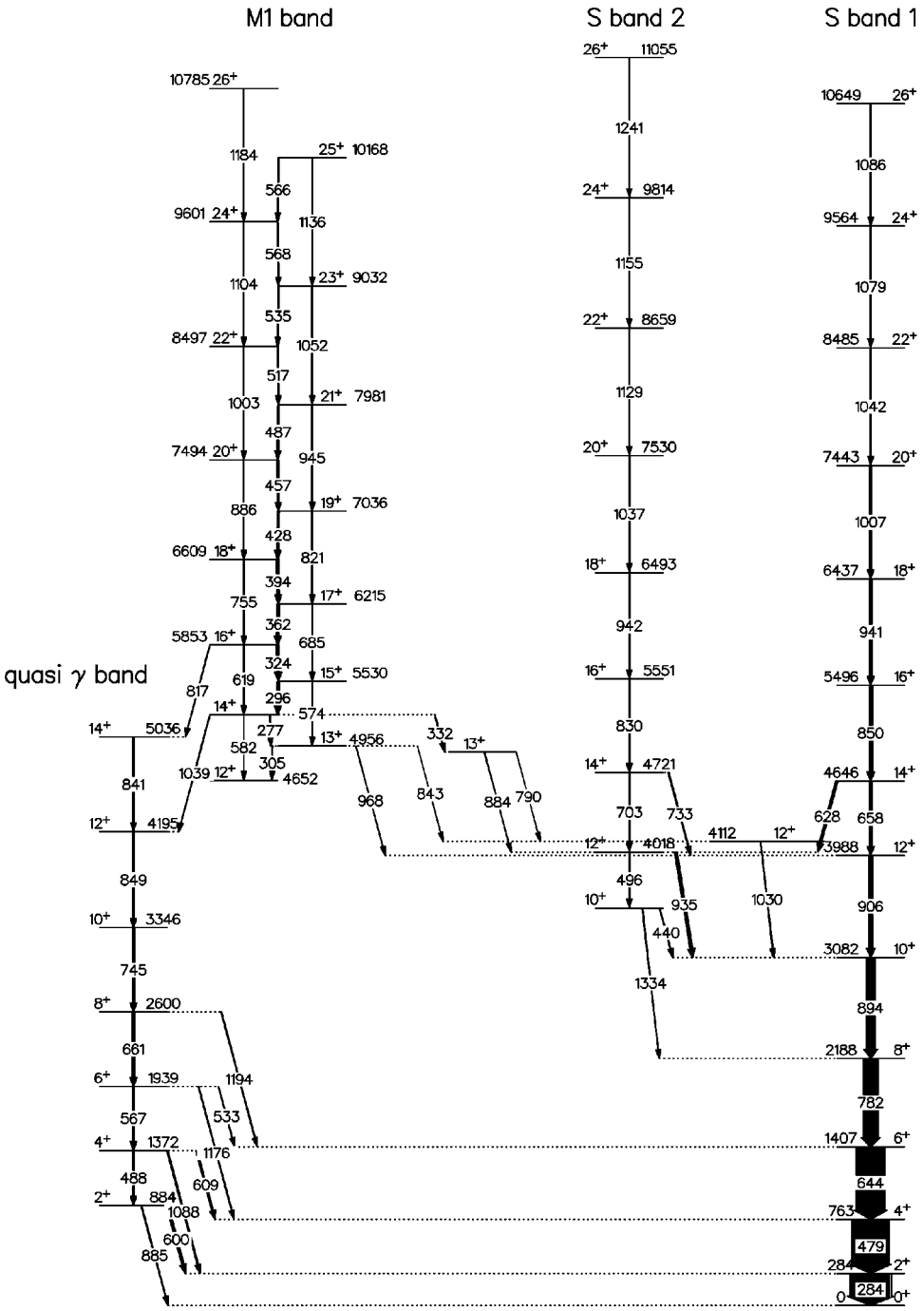

FIG. 1. Partial level scheme of ^{128}Ba as observed in the ^{96}Mo(^{36}S,4n)^{128}Ba reaction, taken from Ref. [3]

II. $\gamma\gamma$ ANGULAR CORRELATION ANALYSIS WITH SpeeDCO

A. Principle of SpeeDCO

In this section we explain the principle and main outline of the SpeeDCO analysis. A detailed description of the method focusing on the sensitivity for spin determination and multipolarity mixing in different contexts will be given in an upcoming publication [10]. In the formulas and conventions we follow Ref. [4]. We call the experimental DCO distribution of a given $\gamma\gamma$ cascade $w(\theta_1,\theta_2,\phi)$. In a conventional DCO analysis, this experimental distribution will be compared to a hypothetical distribution $W(\theta_1,\theta_2,\phi)$ of two γ rays $\gamma_{1,2}$ emitted in a cascade from an oriented nuclear state I_1. $W(\theta_1,\theta_2,\phi)$ is calculated by

$$W(\theta_1,\theta_2,\phi)=\sum_{\lambda_1,\lambda,\lambda_2} B_{\lambda_1}(I_1)A_{\lambda}^{\lambda_1\lambda_2}(\gamma_1)A_{\lambda_2}(\gamma_2) \times H_{\lambda_1\lambda\lambda_2}(\theta_1\theta_2\phi), \quad (1)$$

where

$$H_{\lambda_1\lambda\lambda_2}=\frac{4\pi}{2\lambda_2+1}\sum_{q=-\lambda'}^{q=\lambda'}\langle\lambda_1 0\lambda q|\lambda_2 q\rangle \times Y_{\lambda q}(\theta_1,0)Y^*_{\lambda_2 q}(\theta_2\phi),$$

$$\lambda'=\min(\lambda,\lambda_2). \quad (2)$$

TABLE I. Expansion coefficients used in the SpeeDCO expansion of directional correlations from oriented states. The values given for $A_\lambda^{\lambda_1\lambda_2}$ and A_{λ_2} are maximal absolute values for $\Delta I=0,1,2\,\gamma$ transitions with mixed dipole or quadrupole multipolarity decaying from $I_1=10$. The absolute values for B_{λ_1} are calculated at $I_1=10$ with an orientation parameter $\sigma=4$. The product of the three numbers measures the importance of the expansion term for typical $\gamma\gamma$ cascades. In the last column, a simple description of the angular function $H_{\lambda_1\lambda\lambda_2}$ is given, in cases where it depends on one geometrical parameter only.

		Maximal values (see caption)				
Λ	$\lambda_1\lambda\lambda_2$	B_{λ_1}	$A_\lambda^{\lambda_1\lambda_2}$	A_{λ_2}	Prod.	Geom.
1	0 0 0	1.000	1.000	1.000	1.000	Total statistics
2	0 2 2	1.000	0.404	0.817	0.330	$\propto Pl_2(\angle(\gamma_1,\gamma_2))$
3	0 4 4	1.000	0.186	0.558	0.104	$\propto Pl_4(\angle(\gamma_1,\gamma_2))$
4	2 0 2	0.665	0.440	0.817	0.239	$\propto Pl_2(\theta_2)$
5	2 2 0	0.665	0.365	1.000	0.243	$\propto Pl_2(\theta_1)$
6	2 2 2	0.665	0.205	0.817	0.111	
7	2 2 4	0.665	0.220	0.558	0.081	
8	2 4 2	0.665	0.138	0.817	0.075	
9	4 0 4	0.244	0.317	0.558	0.043	$\propto Pl_4(\theta_2)$
10	4 4 0	0.244	0.186	1.000	0.045	$\propto Pl_4(\theta_1)$
11	4 2 4	0.244	0.140	0.558	0.019	
12	4 4 2	0.244	0.097	0.817	0.019	

The angles $\theta_{1,2}$ denote the polar angles of the emitted $\gamma_{1,2}$ radiation with respect to the beam axis, and ϕ is the difference in the respective azimuthal angles. The tensor $B_{\lambda_1}(I_1)$ describes the orientation of the upper nuclear state, the tensor $A_\lambda^{\lambda_1\lambda_2}(\gamma_1)$ the orientation of the intermediate state due to emission of γ_1, and $A_{\lambda_2}(\gamma_2)$ the emission of γ_2. For the definition of these tensors see Ref. [4].

To clarify the principle of the SpeeDCO analysis, we rewrite Eq. (1) as

$$W(\Theta)=\sum_\Lambda S_\Lambda H_\Lambda(\Theta), \tag{3}$$

where we introduce the indices Θ and Λ, with $\Theta=(\theta_1,\theta_2,\phi)$ standing for the angles of all available N detector pairs of the given spectrometer setup and $\Lambda=(\lambda_1,\lambda,\lambda_2)$ denoting the relevant terms of Eq. (1) (see Table I). Note that S_Λ, which is the product of the A and B tensors, carries all the information about the hypothetical spins and multipolarities. The SpeeDCO analysis is based on the observation that the vectors $H_\Lambda(\Theta)$ form an orthogonal basis of the possible DCO patterns $W(\theta_1,\theta_2,\phi)$. We use this basis to transform the experimental DCO spectra $w_\Theta(E_1,E_2)$ into their Fourier representations $s_\Lambda(E_1,E_2)$ by the expression

$$s_\Lambda(E_1,E_2)=\sum_\Theta \frac{H_\Lambda(\Theta)}{\|H_\Lambda\|} w_\Theta(E_1,E_2) \tag{4}$$

and compare experiment and hypothesis in Fourier space rather than in geometrical space. The normalization with the quotient $\|H_\Lambda\|=\sqrt{1/N\Sigma_\Theta H_\Lambda^2}$ is performed in order to simplify the error calculation discussed in Sec. II D. Calculations show that the 12 expansion coefficients $\Lambda=(\lambda_1\lambda\lambda_2)$ of Table I are sufficient to describe the relevant DCO patterns for dipole and quadrupole radiations [10].

The Fourier transformation [Eq. (4)] is performed for each energy bin (E_1,E_2) of the coincidence spectrum, providing us with 12 two-dimensional histograms of expansion coefficients. A sample coincidence spectrum in four of the expansion matrices is displayed in Fig. 2.

The SpeeDCO method is based on two concepts. The first is the Fourier transformation of DCO patterns via Eq. (4) and the observation that actual correlation patterns of $\gamma\gamma$ cascades are determined by relatively few terms in the expansion. The second concept is to perform this expansion not on fitted peak areas but channel by channel on histograms and to extract the expansion coefficients by fitting peaks and backgrounds to these histograms.

While the first concept is mathematically straightforward, the second relies on the assumption that peaks and the continuous background are governed by the same terms of the expansion. The continuous background of $\gamma\gamma$ spectra emitted in fusion-evaporation reactions consists mainly of two com-

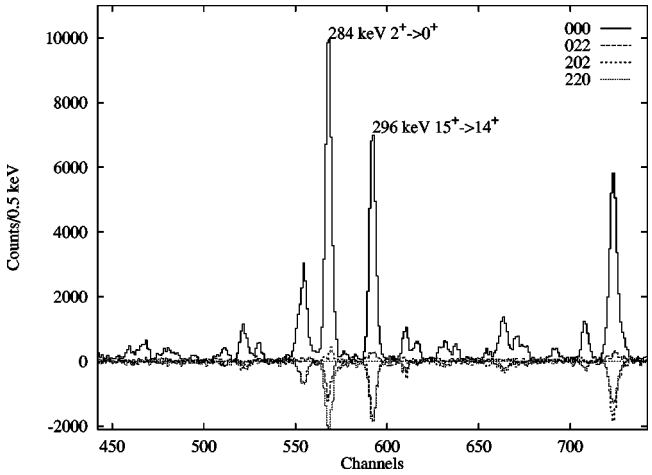

FIG. 2. SpeeDCO spectra gated on the 324 keV transition in the expansion matrices 000, 022, 202, and 220; see text for details.

TABLE II. Sample comparison of DCO analysis and SpeeDCO analysis for the (400,326) keV cascade in the ^{124}Xe experiment at NORDBALL (see text).

Method	Spins	χ^2	σ	δ_1	δ_2
DCO	(17)(16)(15)	0.5	2(1)	−0.13(2)	−0.12(2)
Transformed DCO		0.5	1.2(10)	−0.13(2)	−0.12(2)
SpeeDCO		0.5	0.2(10)	−0.15(2)	−0.14(2)

ponents, i.e., Compton escape signals of the detectors and a quasicontinuum of γ rays from excitation regions with a high level density. Since both types of background have the same angular correlations as discrete γ transitions, we can expect to find in the expansion spectra the same principal behavior for the signal and background as in ordinary spectra.

B. Software development and tests

In order to prove the principle of SpeeDCO and the software developed for it, it was necessary to test the method on a data set where both approaches, i.e., a conventional DCO analysis and SpeeDCO, were possible. This data set was provided by an experiment on the neighboring nucleus ^{124}Xe with the NORDBALL spectrometer at the NBI in Risø. The NORDBALL spectrometer is very favorable for conventional angular correlation studies, since its geometry results in only 12 correlation groups [5]. The results of the conventional DCO analysis for ^{124}Xe will be published in [11].

In Table II we show the results of three different approaches for the DCO analysis of the (400,326) keV cascade from the ^{124}Xe experiment. This cascade is part of a $M1$ band similar to the one measured in ^{128}Ba. The first line presents the result of a conventional DCO analysis [11]. The second line describes the results we obtained after transforming the same peak areas used for the conventional analysis into the SpeeDCO basis. The third line is the result of the full SpeeDCO analysis, i.e., the analysis of the coincidence spectra of expansion coefficients. While the extracted values of δ are consistent within the uncertainty limits, the fitted values for σ seem to be smaller than for the usual DCO analysis. The correct evaluation of the error analysis is, however, difficult because the experiment provides only 12 geometrical groups which are transformed into the 12 expansion groups of SpeeDCO. This situation creates correlations between the values of different expansion groups, which cannot be included in our error analysis. The problem of correlated values disappears for the GASP experiment on ^{128}Ba, where the 12 expansion groups are calculated from 107 independent geometrical values.

C. Data analysis

One convenient property of Eq. (4) is that the 12 spectra $s_\Lambda(E_1,E_2)$ can be incremented event by event, since the summation over the different angles in Eq. (4) can be performed as a summation over events with their individual geometry. For each event (E_1,E_2,Θ), the 12 $s_\Lambda(E_1,E_2)$ are incremented by the value of $H_\Lambda(\Theta)/\|H_\Lambda\|$. This technique requires the use of floating point histograms, which can be rounded out to integer values after all events have been sorted.

D. Error calculation

The uncertainties of the coincidence histograms $s_\Lambda(E_1,E_2)$ can be calculated by straightforward error propagation of the terms in the sum of Eq. (4). In the sorting process, the error matrices

$$e_\Lambda(E_1,E_2)=\sum_\Theta \left(\frac{H_\Lambda(\Theta)}{\|H_\Lambda\|}\right)^2 w_\Theta(E_1,E_2) \tag{5}$$

can be incremented just in the same way as the expansion matrices s_Λ. The uncertainty of an expansion coefficient is then calculated as $\sqrt{e_\Lambda(E_1,E_2)}$. Since these error matrices double the memory required for sorting, we looked for a less resource-consuming procedure. We employed an approximation by replacing the actual counting rate $w_\Theta(E_1,E_2)$ with the average counting rate $w'(E_1,E_2)$ in Eq. (5). The error matrix then equals the total number of events at (E_1,E_2). At this point the normalization condition $\sqrt{\Sigma_\Theta(H_\Lambda(\Theta)/\|H_\Lambda\|)^2}=N$ was used, with N equal to the number of detector pairs. We compared the results of a full error calculation and our approximation on the ^{124}Xe data set described in the previous section. Both methods provide similar results.

E. Efficiency calibration

The efficiency of the individual detectors was calibrated with a mixed source of the ^{152}Eu and ^{133}Ba isotopes placed at the target position. The energy dependence of the detector efficiency was fitted with the five-parameter function $\epsilon(E_\gamma)=A*(E_\gamma-C+D*e^{-E*E_\gamma})^B$.

The calibration was tested on the distribution of several strong ^{128}Ba γ transitions over the individual detectors. We found that the calibrated efficiency overestimated the counting rates of detectors 1–24 relative to 25–40 by a constant factor 1.11. We attribute this difference to dead time effects of the data acquisition system, which employs two multiplexed analog-to-digital converters (ADC's) for detectors 1–24 and 25–40, respectively. Thus we reduced the efficiency calibrations of detectors 1–24 by a factor of 1.11 without changing the energy dependence. This correction removes mainly a forward-backward asymmetry of the observed reaction counting rates. For the thick target spectra we furthermore had to correct the calibrated efficiencies for absorption in the bismuth backing.

F. Spectra analysis and comparison to hypotheses

To support the analysis of multiple coincidence matrices, we developed the program CLAYMORE, which generates gated spectra in all matrices along with the respective error spectra. The background subtraction in the two-dimensional

matrices is performed following the method of Ref. [12] by assigning a continuous background to the matrix projections. This background is generated by linear interpolation of manually selected regions. The same regions are used for the projections of all expansion matrices. The two-dimensional background hypothesis is then calculated as

$$b_{2d}(E_1,E_2)=p_x(E_1)*b_y(E_2)+b_x(E_1)*p_y(E_2)+b_x(E_1)*b_y(E_2),$$

where $p_{x,y}$ stand for the background-subtracted projection spectra and $b_{x,y}$ for the continuous background hypotheses of respective projections.

A sample of background-subtracted expansion spectra gated on the 324 keV transition is displayed in Fig. 2. As expected, the expansion spectra show Gaussian peaks with varying relative amplitudes.

The peak areas are extracted from these gated spectra by simultaneously fitting a selected region with a number of Gaussian peaks over an optional constant or linear background. This additional background hypothesis was introduced in order to be independent of local deviations from the global background subtraction pattern described above. The extracted peak areas proved to be reliable and not very sensitive to variations in the gate and background parameters.

In a second step of the analysis, the peak areas for a given $\gamma\gamma$ cascade are compared to calculated patterns of different spin hypotheses and multipolarity mixing ratios δ with the program CORLEONE.

With ''ideal'' 4π spectrometers the transformation of Eq. (4) is exact in the sense that experimental s_Λ coefficients can be directly compared to the hypothetical S_Λ one. In real experimental setups, effects such as varying detector efficiencies or geometrical biases of the spectrometer cause slight nonorthogonalities in the basis $H_\Lambda(\Theta)$. To correct for detector efficiencies during the sorting process would increase the data-processing time of an individual event substantially. Thus, we chose to calculate these effects together with the theoretical hypotheses, which is easier to do.

III. RESULTS FOR THE ^{128}Ba EXPERIMENTS

A. Tests and systematic errors

The SpeeDCO analysis was performed on the thick and thin target data from the GASP experiments on ^{128}Ba. We first analyzed the SpeeDCO pattern of high-statistics $\gamma\gamma$ cascades from the thick target experiment, which provide an excellent test for possible systematic problems in the analysis. After the correction for the efficiency calibration discussed above, the experimental expansion pattern of the $4^+\rightarrow 2^+\rightarrow 0^+$, 479–284 keV cascade could be reproduced within a few percent in the calculation. The expansion pattern together with the fitted hypothesis is displayed in Fig. 3. Note that for the actual spin and multipolarity assignments presented in the following section, the error calculation is dominated by the statistical limits of the experiment, not by systematic uncertainties.

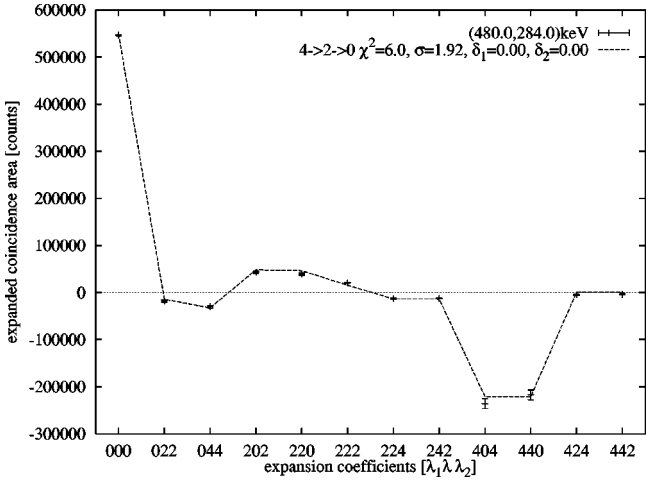

FIG. 3. Correlation pattern of the (479,284) keV cascade in the ground state band of ^{128}Ba. The dashed line represents a least squares fit to the observed SpeeDCO pattern with the orientation parameter $\sigma=1.83(7)$. The calculated pattern agrees within deviations of $\pm 3\%$ of the total statistics.

B. Mixing ratios in the ''$M1$ band''

The experimental SpeeDCO pattern of the (324,296) keV cascade together with the adopted hypothesis is shown in Fig. 4. The figure also presents a hypothetical pattern for the local χ^2 minimum of the parameters $\sigma=4.2$, $\delta_1=3.60$, and $\delta_2=3.60$ as well as the pattern for a pure dipole cascade.

Figure 5 displays the χ^2 analysis for the independent variation of both δ values for the (324,296) keV cascade of the ''$M1$ band.'' In the calculation, the orientation parameter σ was varied independently to minimize the χ^2 value at every (δ_1,δ_2) point. The calculation reveals a unique minimum at the parameters $\sigma=2.0(16)$, $\delta_1=-0.20(3)$, and $\delta_2=-0.17(4)$ with a χ^2 value of 1.7. The other local minima have larger values, e.g., $\chi^2\geqslant 4$.

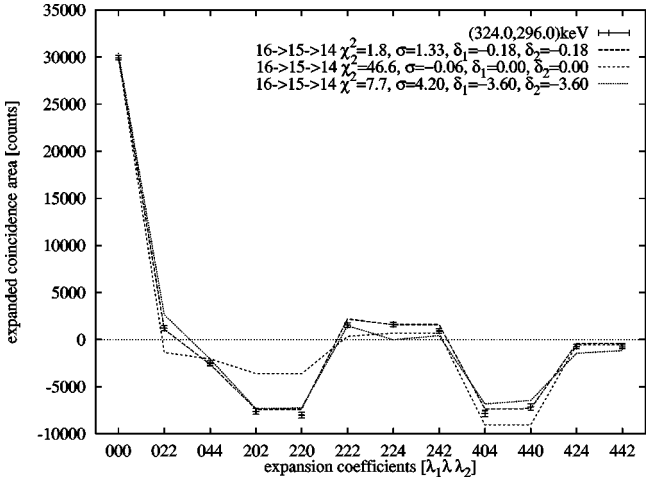

FIG. 4. Correlation pattern of the (324,296) keV cascade in the ''$M1$ band'' of ^{128}Ba. The dashed line represents the accepted hypothesis with the parameters $\sigma=1.8$, $\delta_{324}=-0.18$, and $\delta_{296}=-0.18$. The second hypothesis (short dashed line) represents a χ^2 fit with the assumption of pure dipole character. The third hypothesis (points) corresponds to a local minimum in the χ^2 surface of Fig. 5.

TABLE III. $\delta(E2/M1)$ values from the SpeeDCO analysis for members of the ''$M1$ band'' in ^{128}Ba.

I_i^π	E_γ [keV]	$\delta(E2/M1)$
13^+	305	$-0.19(9)$
14^+	277	$-0.14(4)$
15^+	296	$-0.18(3)$
16^+	324	$-0.18(3)$
17^+	362	$-0.20(3)$
18^+	394	$-0.24(3)$
19^+	428	$-0.22(5)$
20^+	457	$-0.20(4)$
21^+	487	$-0.18(7)$

The analysis of the correlation patterns for the members of the ''$M1$ band'' provided $E2/M1$ mixing ratios for eight $\Delta I=1$ transitions between $-0.14(4)$ and $-0.24(5)$. To obtain a value for the mixing ratio, the angular correlations between the transition in question and its upper and lower neighboring $\Delta I=1$ transitions were analyzed and the fitted value averaged over both results. Correlations with the much weaker $\Delta I=2$ transitions and correlations with second next neighboring $\Delta I=1$ transitions were analyzed in order to verify these values independently. The values obtained with different methods are consistent within the statistical uncertainties. The results of these fits are presented in Table III.

C. Spin determination

The decay out of the ''$M1$ band'' to both S bands and the quasigamma band is spread out over six one- and two-step decay paths [3]. The observed connections limit the possible spin hypotheses for the ''$M1$ band'' to $\pm 1\hbar$. The assignment of negative parity in [3] was based on the identification of the band with the negative parity band predicted by TAC calculations.

We analyzed the correlations of the (277,968) and (277,843) keV cascades, which correspond to the decay out of the ''$M1$ band'' feeding two different 12^+ states of the ground state and the first S band (see Fig. 1 and Table IV). From the SpeeDCO analysis we can exclude the $\Delta I=0$ character proposed by Ref. [3] and establish a $\Delta I=\pm 1$ character

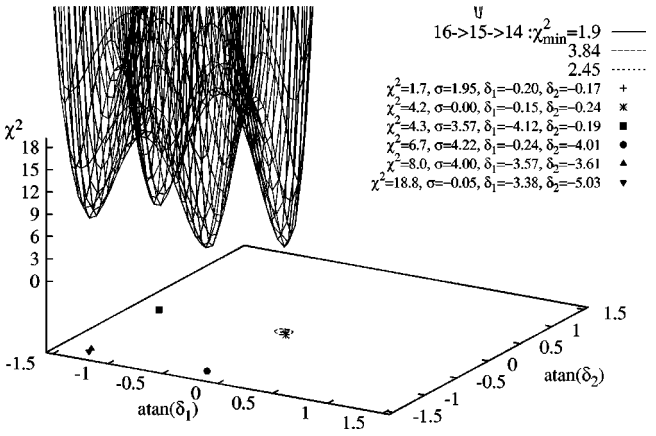

FIG. 5. χ^2 analysis of the SpeeDCO pattern of the (324,296) keV cascade in the ''$M1$ band'' of ^{128}Ba. During the variation of the parameters δ_{324} and δ_{296}, the orientation parameter σ was minimized independently at each point.

for the 968 and 843 keV transitions. We assume that the lower-spin hypothesis is rather unlikely, because it would place the $M1$ band so far above the yrast band that it would hardly be populated in the reaction. The SpeeDCO pattern of the (277,968) keV cascade together with the least squares fits for the spin hypotheses in question is displayed in Fig. 6.

Since we can exclude the observation of $M2$ transitions competing with collective in-band $M1/E2$ transitions, the previous assignment also determines positive parity for the $M1$ band. The 1039 keV and 817 keV γ rays connecting the ''$M1$ band'' and the quasigamma band are $E2$ transitions. The other angular correlations of γ rays associated with the decay out of the $M1$ band are all consistent with this new assignment.

IV. DISCUSSION

A. Sensitivity of the SpeeDCO method

The presence of mixed transitions with comparable $E2$ and $M1$ content leads to strong and characteristic DCO patterns, which often allow unique spin and multipolarity assignments even for weak cascades. Thus, DCO is most sensitive as a method to determine spins when mixed $E2/M1$

TABLE IV. SpeeDCO analysis to determine spin and parity of the magnetic dipole band. The three transitions at 968, 938, and 847 keV connect the 4956 keV level with the 12^+ states of the ground state and the proton and neutron S bands. The correlations of each transition independently confirm the $\Delta I=1$ assignment. The other hypotheses with $\Delta I=0$ can be excluded by their χ^2 values.

(E_1, E_2)	$I_1 \to I_2 \to I_3$	δ_2	χ^2
(277,968)	$13^+ \to 12^+ \to 12^+$	$-5.4^{+3.8}_{-\inf}$	3.3
	$13^- \to 12^- \to 12^+$	0	6.3
	$\boxed{14^+ \to 13^+ \to 12^+}$	$\boxed{-0.6^{+0.6}_{-1.4}}$	$\boxed{0.5}$
(277,843)	$13^+ \to 12^+ \to 12^+$	$-5.4^{+3.6}_{-\inf}$	6.9
	$13^- \to 12^- \to 12^+$	0	10.3
	$\boxed{14^+ \to 13^+ \to 12^+}$	$\boxed{-1.5^{+0.7}_{-3}}$	$\boxed{1.0}$

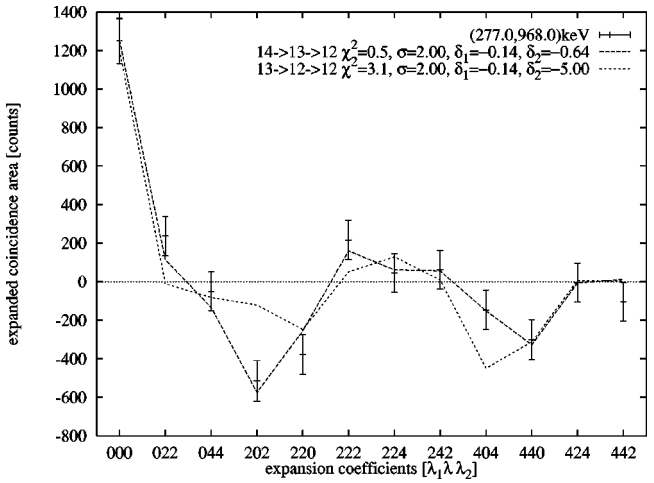

FIG. 6. Experimental SpeeDCO pattern of the (277,968) keV cascade depopulating the ''$M1$ band'' together with the theoretical patterns for the two possible spin hypotheses. The spin assignment provided by the first hypothesis was accepted.

transitions are in a cascade with the transitions of unknown spins. A good illustration is the spin assignment for the ''$M1$ band'' discussed in the previous section. Only the correlation of the mixed $E2/M1$ in-band transition with the mixed $E2/M1$ decay out had a sufficiently characteristic DCO pattern to decide between the possible spin hypotheses. In contrast, the $E2$ decay through the 1039 keV transition to the quasigamma band, although twice as strong, can be fitted equally well with $\Delta I=1$ and $\Delta I=0$ hypotheses.

To demonstrate the advantage of the SpeeDCO analysis over the conventional gated angular distributions, the same (324,296) keV cascade of Fig. 5 was analyzed with the terms corresponding only to the Legendre polynomial Pl_2 and Pl_4 angular distribution coefficients of both γ transitions (see Table I and Fig. 7). From the gated angular distribution analysis alone, no unique solution for δ_1 or δ_2 can be found. This is due to the fact that the angular distribution is determined by a product of the free parameters σ and δ. Only if the statistics are sufficient to determine the Pl_4 coefficient can this ambiguity be resolved in angular distribution measurements.

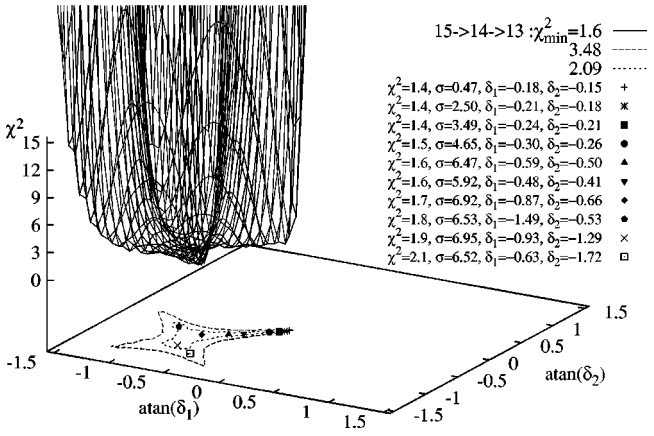

FIG. 7. Same hypothesis as in Fig. 5, but χ^2 only based on angular distribution analysis, demonstrating that no unique χ^2 minimum can be found.

The additional information of a correlation analysis can be most easily demonstrated with the (022) angular function [Eq. (2)], which depends only on the relative angle between both γ rays (see Table I). Therefore, the calculated coefficients of this term are independent of the orientation parameter σ and depend only on the δ values and spins of both transitions.

B. Examination of rotational transitions

The experiments on ^{128}Ba with the GASP spectrometer revealed a wealth of data on the ''$M1$ band'' in this nucleus [3]: the branching ratios between $\Delta I=1$ and $\Delta I=2$ transitions were measured and compared to predictions of the TAC model and of a high-K rotational band. For three band members, lifetimes could be obtained by the Doppler-shift attenuation method (DSAM).

The determination of positive parity in our work leads us to assign a $(\pi h_{11/2})^2\times(\nu h_{11/2})^2$ configuration to the ''$M1$ band.'' The positive parity creates additional problems for the TAC description in [1]. As was pointed out in Ref. [3], the TAC predictions for positive parity do not match the experimental data of branching ratios and matrix elements.

Another open question of Ref. [3] was the assumption of pure $M1$ character for the $\Delta I=1$ transitions. Our measured values of $\delta\approx-0.2$ correspond to an $M1$ content of $1/(1+\delta^2)\approx 96\%$, which results only in minor corrections of the previous results.

In previous works on $M1$ bands, the $B(M1)_{\Delta I=1}/B(E2)_{\Delta I=2}$ branching ratio was employed to investigate the picture of magnetic rotation vs collective rotation. This observable cannot tell us if $B(E2)$ values increase or if $B(M1)$ rates decrease with spin. These features correspond to the pictures of a high-K rotational band or a shears band, respectively. So far, the absolute matrix elements were only in few cases measured with sufficient precision to discriminate between both pictures.

Measuring the mixing ratio $\delta(E2/M1)$ provides us with an additional observable to test the character of rotational matrix elements. To show this, we calculate the matrix elements of a rotational band according to Ref. [13]. For $K\neq 1/2$ the $B(E2)_{\Delta I=2}/B(M1)_{\Delta I=2}$ branching ratios are

$$\frac{B(E2)_{\Delta I=2}}{B(M1)_{\Delta I=1}} = \frac{5}{12}\frac{(eQ_0)^2}{[(g_k-g_R)\mu_N]^2}\frac{3(I_1+K-1)(I_1-K-1)}{K(2I_1-1)(2I_1-2)}. \qquad (6)$$

The calculation predicts a stronger reduction of $B(E2)_{\Delta I=2}$ than of $B(M1)_{\Delta I=1}$ in the vicinity of the bandhead, which leads to the observed large $M1$ branchings.

With the matrix elements of Ref. [13] the mixing ratio $\delta(E2/M1)$ is calculated as

$$\delta = 0.933E_\gamma\frac{\langle I_1-1\|O(E2)\|I_1\rangle}{\langle I_1-1\|O(M1)\|I_1\rangle} = 0.933E_\gamma[(I_1-1)(I_1+1)]^{-1/2}\frac{Q_0}{(g_k-g_R)}, \qquad (7)$$

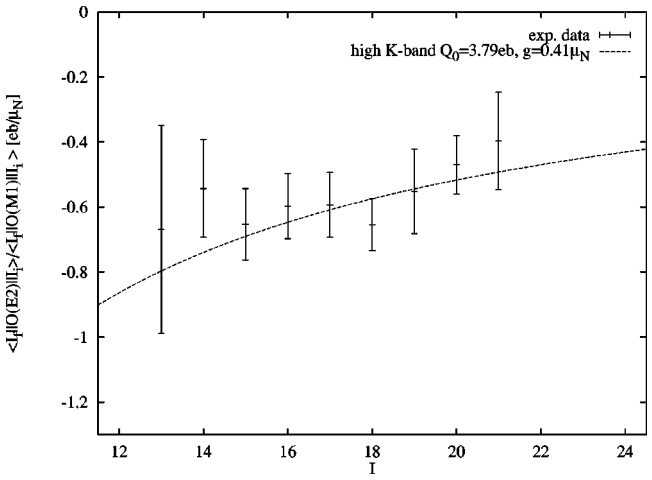

FIG. 8. Experimental values for $\langle I_i-1\|O(E2)\|I_i\rangle/\langle I_i-1\|O(M1)\|I_i\rangle$ extracted with Eq. (7) for transitions in the ''$M1$ band'' in ^{128}Ba. The data are compared to a fit with the matrix elements of a rotational band with the effective charges $Q_0=3.79\ e$ b, $|g_K-g_R|=0.41$. These values were fitted in Ref. [3] to the $B(M1)/B(E2)$ branching ratios and to the lifetimes of the lowest three band members.

where E_γ is in units of MeV, Q_0 in e b, and (g_K-g_R) in μ_N. We find that, unlike the $\Delta I=2/\Delta I=1$ branching ratios, the mixing ratio calculated for a rotational band is *independent* of the K quantum number and, thus, is a more direct observable for the ratio of the effective $E2$ and $M1$ charges.

In Ref. [3] the branching ratios and level lifetimes were fitted with the matrix elements of a high-K rotational band and the parameters $|Q_0|=3.79(21)\ e$ b $[\equiv\beta=0.24(1)]$, $|g_K-g_R|=0.41(2)\mu_N$, and $K=9.4(3)$. We extracted the matrix elements $\langle I_1-1\|O(E2)\|I_1\rangle/\langle I_1-1\|O(M1)\|I_1\rangle$ from the measured $\delta(E2/M1)$ using Eq. (7). In Fig. 8 these experimental values are compared to the values calculated for a high-K band with the parameters of [3]. The good agreement provides an additional, sensitive test for the ratio of the fitted $|Q_0|$ and $|g_K-g_R|$ values.

V. CONCLUSION

We performed for the first time a full DCO analysis on the data of a GASP experiment. Our new analysis method, which we call spectral expansion of DCO (SpeeDCO), is applicable to 4π spectrometers such as GAMMASPHERE or EUROBALL, where a conventional DCO analysis is not possible. The use of $\gamma\gamma$ correlations increases the sensitivity to determine spins and multipolarities significantly over the method of gated angular distributions and allows for unique measurements even in weakly populated bands. The multipolarity mixing ratios, which we measured in the ''$M1$ band'' of ^{128}Ba, are consistent with the picture of a high-K rotational band.

ACKNOWLEDGMENTS

The authors would like to thank the authors of [11] for providing the data on ^{124}Xe and A. O. Macchiavelli for the fruitful discussions concerning the physics of mixing ratios. Work at the IKP Köln is partially supported by the German BMBF under Contract No. 06OK668. Work at ANL is supported by the U.S. DOE, Nuclear Physics Division, under Contract No. W-31-109-ENG-38.

[1] F. Dönau, S. Frauendorf, O. Vogel, A. Gelberg, and P. von Brentano, Nucl. Phys. **A584**, 241 (1995).
[2] S. Frauendorf, Nucl. Phys. **A557**, 259c (1993).
[3] O. Vogel *et al.*, Phys. Rev. C **56**, 1388 (1997).
[4] K. S. Krane, R. M. Steffen, and R. M. Wheeler, Nucl. Data Tables **11**, 5 (1973).
[5] L. P. Ekström and A. Nordlund, Nucl. Instrum. Methods Phys. Res. A **313**, 421 (1992).
[6] I. Wiedenhöver, J. Yan, U. Neuneyer, R. Wirowski, P. von Brentano, A. Gelberg, N. Yoshida, and T. Otsuka, Nucl. Phys. **A582**, 77 (1995).
[7] I. Wiedenhöver, A. Gelberg, N. Pietralla, J. Gableske, A. Dewald, and P. von Brentano, Phys. Rev. C **56**, R2354 (1997).
[8] D. Bazzacco, in *Proceedings of the International Conference on Nuclear Structure at High Angular Momentum*, Ottawa, 1992, edited by R. Andrews, J. Cameron, T. Drake, S. Pilotte, D. Radford, J. Waddington, and D. Ward (AECL Research, Chalk River, Ontario, 1992), Vol. 2.
[9] I. Y. Lee, in *Proceedings of the Conference on Nuclear Structure in the Nineties*, edited by N. R. Johnson [Nucl. Phys. **A520**, 641c (1990)].
[10] I. Wiedenhöver, Nucl. Instrum. Methods Phys. Res. A (to be published).
[11] I. Schneider *et al.* (unpublished).
[12] D. C. Radford, Nucl. Instrum. Methods Phys. Res. A **361**, 306 (1995).
[13] A. Bohr and B. Mottelson, *Nuclear Structure II* (Benjamin, Reading, MA, p. 975).